CRYSTAL GROWTH & DESIGN

pubs.acs.org/crystal

Article

Strontium-Substituted α-TCP: Structure, Stability, and Reactivity in Solution

Massimo Gazzano, Katia Rubini, Adriana Bigi, and Elisa Boanini*

Cite This: *Cryst. Growth Des.* 2023, 23, 5690−5698

Read Online

ACCESS | Metrics & More | Article Recommendations | Supporting Information

ABSTRACT: α-Tricalcium phosphate (α-TCP) is widely used as a component of bone cements, and many efforts have been made to dope it with strontium ion (Sr), which is known for its beneficial role in bone tissue. However, the range of possible substitution of strontium for calcium (Ca) into α-TCP, as well as its effect on the α-TCP structure, has not been clarified yet. Herein, we investigate this substitution through the examination of α-TCP synthesized at high temperatures in the presence of increasing amounts of strontium according to two different routes: *1-step* and *2-steps*. The results show that Sr can enter into an α-TCP structure up to about 10 atom % and substitutes for calcium mostly at specific cation sites, namely, M(5), M(11), and M(17), characterized by relatively low bond valence sums and long mean Ca−O distance. Strontium presence stabilizes α-TCP delaying its transformation into octacalcium phosphate and hydroxyapatite in H_3PO_4, as well as in physiological solution. Although the two methods of synthesis provide similar structural results, the products of *1-step* synthesis display a slightly smaller crystallite size and greater solubility and, as a consequence, a faster hydrolysis reaction.

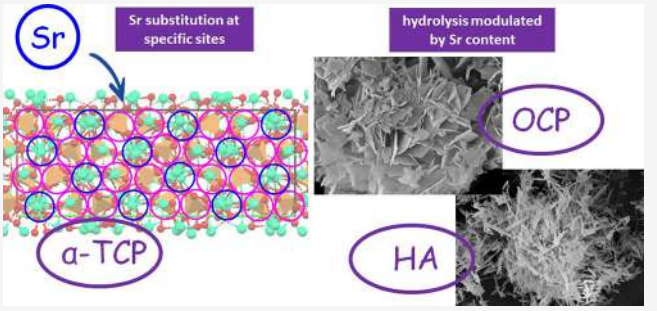

INTRODUCTION

Crystalline tricalcium phosphates, $Ca_3(PO_4)_2$, include three polymorphs characterized by a Ca/P molar ratio of 1.5 but different thermal stability. Rhombohedral β-TCP (space group *R3c*) is stable up to 1120 °C,[1] monoclinic α-TCP (space group $P2_1/a$) is stable between 1120 and 1430 °C and metastable at room temperature,[2−4] whereas between 1430 and 1765 °C, the stable polymorph is α′-TCP, which cannot maintain its stability at room temperature.[4]

Both β- and α-TCP are of great interest from a biological point of view and are utilized in the preparation of biomaterials for hard tissue repair.[5,6] Poorly crystalline hydroxyapatite, as well as biological apatites, converts partially into β-TCP by heat treatment,[7] and β-TCP is an osteoconductive and osteoinductive bioresorbable ceramic.[8] α-TCP is more soluble than β-TCP (pK_{sp}: 25.5 vs 28.9), and at physiological values of pH and temperature, it hydrolyzes to calcium-deficient hydroxyapatite.[9,10] These are the main reasons why, although α-TCP is not present in biological tissues, it is widely used as a component of bone cements.[6,11] The monoclinic unit cell of α-TCP contains 24 formula units with 72 calcium atoms distributed in 18 independent cation sites.[12] The structure consists of calcium and phosphate (PO_4) ions arranged in columns along the [001] direction: C−C columns containing just Ca cations and C−A columns containing both Ca cations and PO_4 anions.[2] The most common methods of synthesis of α-TCP are by the solid-state reaction of solid precursors at high temperatures and by the heat treatment of a precursor with a Ca/P molar ratio of 1.5.[10,13,14] Thermal treatment of β-TCP at temperatures higher than 1130 °C is the most direct route to get α-TCP.[4] The transformation from β to α-TCP involves a significant reorganization of the crystal structure, which justifies the great amount of energy required for the transformation. On the other hand, the synthesis of the α form by heat treatment of β-TCP often leads to a partial α-β reversal, which has been ascribed to the presence of impurities and/or to the cooling rate.[3,15]

Ionic substitution is a further important parameter in the thermodynamic equilibrium between the two stable polymorphs of TCP.[3] It is known that Mg substitution for Ca stabilizes β-TCP, increasing its thermal stability and preventing its complete transformation into the α phase by heat treatment.[5,16,17] A similar influence was reported for Zn and Sr ions.[18,19] In particular, Jegou Saint-Jean et al. were not able to avoid the presence of a small amount of β-TCP even by raising the temperature of solid-state synthesis of α-TCP to 1500 °C.[19] Sr-doped α-TCP was obtained through a synthesis in solution at room temperature in the presence of small amounts of Sr up to 5 at % and successive heat treatment at 650 °C.[20] However, raising

Received: March 24, 2023
Revised: June 22, 2023
Published: July 3, 2023

https://doi.org/10.1021/acs.cgd.3c00358
Cryst. Growth Des. 2023, 23, 5690−5698

the heat treatment temperature up to 700 °C provoked the appearance of β-TCP as a secondary phase.

In recent years, strontium has been arousing much interest in research due to its significant activity in bone metabolism.[21] In this light, strontium substitution in calcium orthophosphates (CaPs) is of utmost relevance since it has been shown that the beneficial role of this ion in bone cells is maintained when it is coupled with CaPs.[22−25] In particular, Sr-substituted CaPs have been reported to enhance osteoblast viability and differentiation and to inhibit osteoclast proliferation and activity, which must be reduced in pathologies characterized by abnormally high bone resorption. Strontium substitution to calcium of about 13 at % in hydroxyapatite (HA) was reported to almost double osteoblast proliferation in comparison with pure HA,[26] whereas even smaller strontium contents were found to increase significantly the expression of collagen and alkaline phosphatase and to reduce osteoclast proliferation.[27,28] Moreover, a strontium content of about 6 at % in both monetite and brushite determined a remarkable decrease in the production of cathepsin and tartrate-resistant acid phosphatase.[25]

In this study, we report the results of a study on the ability of the α-TCP structure to host strontium substitution for calcium. In particular, the present study investigates the range of possible substitution, as well as the influence of the foreign ion on the α-TCP structure and hydrolysis. To this aim, we followed two different routes of synthesis in the presence of increasing Sr content: (a) heat treatment of β-TCP at 1300 °C (*2-steps*) and (b) direct solid-state reaction at 1300 °C (*1-step*). The hydrolysis behavior of the products was investigated in H_3PO_4 and in saline solution at different temperatures.

MATERIALS AND METHODS

Synthesis Procedures. α-TCP was obtained through the solid-state reaction following two different procedures, as reported in Scheme 1: (a) in *2-steps* by thermal conversion of β-TCP; (b) in *1-step* by the direct solid-state reaction.

For the *2-step* synthesis, the first step consisted in thoroughly grinding by hand a mixture of calcium carbonate, $CaCO_3$ (Carlo Erba, Milan, Italy), and calcium phosphate dibasic dihydrate, $CaHPO_4{\cdot}2H_2O$ (Carlo Erba, Milan, Italy), in the molar ratio of 1:2 and heating it to 1000 °C using a heating ramp of 7°/min and keeping the temperature for 5 h. The result of this first step is the preparation of pure β-TCP powder.[29] Afterward, the powder was extracted, finely ground by hand, heated to 1300 °C using a heating ramp of 7°/min, and the temperature was maintained for 2 h.

Scheme 1. Scheme Illustrates the Two Different Procedures Utilized To Synthesize α-TCP and Sr-Substituted α-TCP

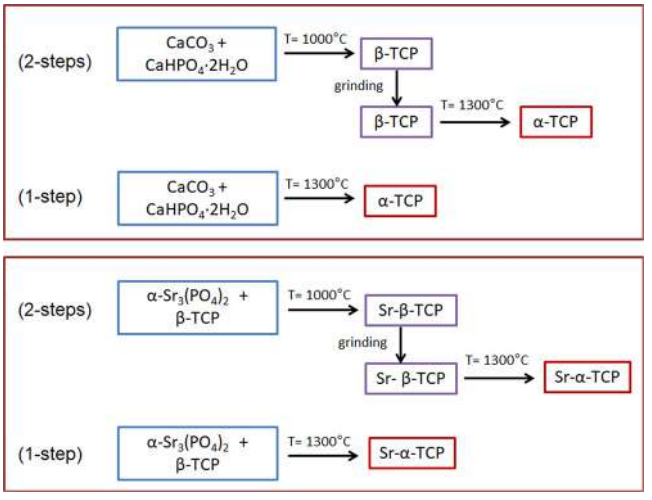

The *1-step* synthesis was performed by thoroughly grinding by hand a mixture of $CaCO_3$ and $CaHPO_4{\cdot}2H_2O$ in the molar ratio of 1:2 and heating it directly to 1300 °C using a heating ramp of 7°/min and keeping the temperature for 2 h.

Now onward, the samples prepared through *2-step* or *1-step* procedures will be labeled as α-TCP or α-TCP-D, respectively.

Strontium substitution in α-TCP was performed using both the *2-step* and the *1-step* procedure.

In the *2-step* procedure, Sr-substituted β-TCP samples were prepared first, and then, Sr-substituted α-TCP samples were obtained by thermal conversion of the Sr-substituted β-TCP samples upon heating to 1300 °C using a heating ramp of 7°/min and keeping this temperature for 2 h. For the preparation of Sr-substituted β-TCP, α-strontium phosphate (α-$Sr_3(PO_4)_2$) was obtained by the solid-state reaction of a mixture of strontium carbonate ($SrCO_3$, Carlo Erba, Milan, Italy) and ammonium phosphate ($(NH_4)_2PO_4$, Carlo Erba, Milan, Italy) in the molar ratio of 3:2, heated at 1200 °C using a heating ramp of 7°/min, and the temperature was maintained for 12 h. Sr-substituted β-TCP samples, with a Sr content up to 80 atom % (respect to total cations Ca + Sr), were prepared by heat treatment of an appropriate stoichiometric mixture of β-TCP and α-$Sr_3(PO_4)_2$, at 1000 °C using a heating ramp of 7°/min, and the temperature was maintained for 12 h.

In the *1-step* procedure, the Sr-substituted α-TCP samples were directly synthesized by mixing the pure β-TCP with the α-$Sr_3(PO_4)_2$ precursor and heating it directly to 1300 °C using a heating ramp of 7°/min and keeping the temperature for 2 h, thus avoiding the intermediate step to substituted β-TCP.

Now onward, the samples synthesized by the *2-step* procedure in the presence of increasing Sr content were labeled SrX, where X indicates the number of Sr atom % with respect to the total cations: $[Sr^{2+}/(Ca^{2+} + Sr^{2+})] \times 100$. Similarly, the samples prepared through *1-step* synthesis will be labeled as SrX-D.

All syntheses were performed in triplicate.

Hydrolysis Reactions. Three types of working conditions were used to study the reactivity in aqueous solution: (a) in 0.0016 M phosphoric acid (H_3PO_4, Carlo Erba, Milan, Italy) solutions, with a starting pH adjusted to 6 using ammonium hydroxide (NH_4OH, Carlo Erba, Milan, Italy), at 25 °C; (b) in 0.0016 M H_3PO_4 solutions, with a starting pH adjusted to 6 using NH_4OH (Carlo Erba, Milan, Italy), at 60 °C; (c) in physiological saline solution (9.0 g/L of sodium chloride-NaCl, Carlo Erba, Milan, Italy), at 60 °C.

Hydrolysis reactions were performed on 100 mg of selected samples incubated in 50 mL of solution under stirring (300 rpm) for different periods of time, up to 7 days. Then, the products were filtered, repeatedly washed with double distilled water, and dried at 37 °C overnight. All sample powders were ground by hand and sieved (<125 μm) before being submitted to hydrolysis.

Characterization. XRD patterns were collected with a PANalytical X'Pert PRO powder diffractometer in the Bragg−Brentano geometry with the following setup: Cu Kα radiation (40 mA, 40 kV), 1/2° slits, X'Celerator detector. Qualitative scans were collected for 40 s at each 0.05° step in the 2θ range 3°−60°; patterns for structural refinements were integrated for 400 s every 0.0167° step, in the interval of 10°−100°.

Rietveld refinements were carried out by means of High Score Plus program, rev. 4.9 by Malvern Panalytical employing scattering factors of Ca^{2+}, Sr^{2+}, P^{5+}, and O^{2-} ions. The bond valence sums (BVS) were calculated for all the cation sites in Sr-substituted α-TCP, assuming a bond valence parameter for the cation of 1.967, which is the value for the Ca^{2+} cation in oxides.[30]

Morphological investigation was performed using a Hitachi S-2400 scanning electron microscope operating at 18 kV. Sputter-coating with gold was performed before examination.

Release of calcium in solution was monitored by incubating α-TCP samples prepared in *2-steps* or *1-step* in physiological solution (NaCl 0.9%) at 60 °C up to 6 h. Measurements were performed by an ICP-OES spectrometer (ICP Optima 4200DV, Perkin Elmer). The calibration line was made with 4 calibration standards (Ca: 0.5, 5, 10,

https://doi.org/10.1021/acs.cgd.3c00358
Cryst. Growth Des. 2023, 23, 5690−5698

and 20 mg/L), prepared by dilution of 1000 mg/L calcium standard solution (VWR International, Milan), in 0.5 M HNO_3. Results from this analysis represent the mean value of three different determinations.

RESULTS AND DISCUSSION

Synthesis. Strontium can replace calcium in the structure of β-TCP, provoking a linear expansion of the lattice parameters, in agreement with the bigger ionic radius of Sr^{2+} than Ca^{2+}.[29] The *2-step* synthesis utilized in this work to obtain α-TCP and Sr-substituted α-TCP consists of heat treatment at 1300 °C of β-TCP and Sr-substituted β-TCP. The powder X-ray diffraction patterns of the products indicate that the method allows one to get α-TCP as a single phase up to a Sr content of 10 at %. Indeed, the patterns reported in Figure 1 show only the presence of α-TCP (ICDD PDF 01-070-0364) up to 10 at % of strontium, whereas the patterns of the samples at a greater Sr content display the presence of a second phase, identifiable as β-TCP (ICDD PDF 01-070-2065). No peaks of α-TCP can be detected in the patterns of samples at a Sr content greater than 15 at %, which show just the X-ray reflections of β-TCP. The lattice constants of the different products increase as a function of the Sr content (Table 1), coherently with the increase of the cation radius (ionic radius: Sr = 0.118 nm; Ca = 0.100 nm). Figure S1 shows that the values of the lattice parameters vary almost linearly with the strontium content. However, in agreement with the different shifts observed for different peaks (Figure 1), the substitution has dissimilar influence on the three parameters: the main effect is on the *b*-parameter, which increases more than the *c*-parameter, whereas the *a*-parameter displays a slight reduction.

The *1-step* synthesis, that is, the solid-state reaction at 1300 °C of a mixture of β-TCP and α-$Sr_3(PO_4)_2$, yields very similar

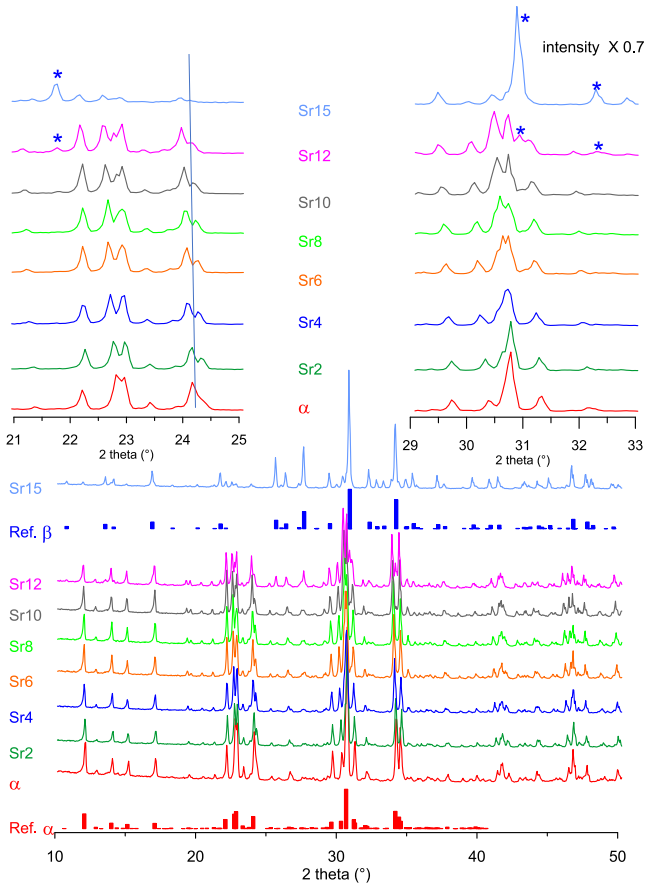

Figure 1. Powder X-ray diffraction patterns of the products obtained by the *2-step* synthesis on the increasing strontium content. At the top, a zoomed view of selected regions of the patterns; the range 29−33° is shown with intensities reduced by a factor of 0.7 compared to those in the range 21−25°; the asterisk symbol highlights most intense β-TCP peaks. Histograms are representation of peak intensities in α-TCP (red)[2] and strontium-substituted β-TCP (blue).[29]

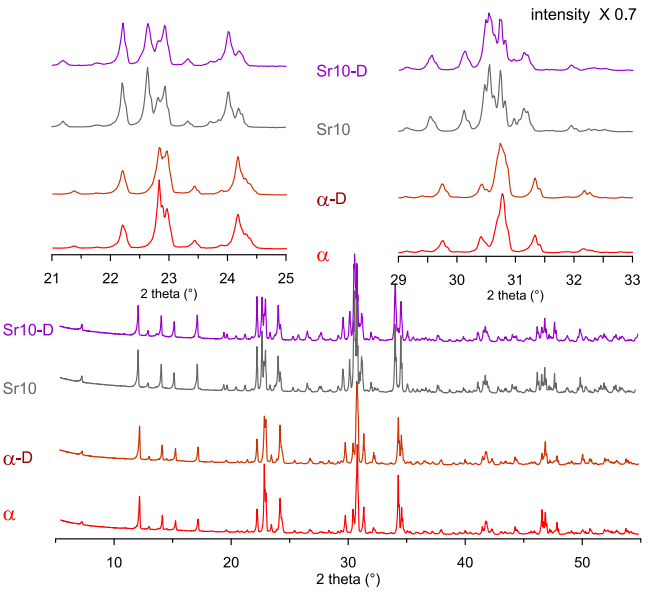

Figure 2. Comparison between powder X-ray diffraction patterns of the samples obtained by one-step and two-step synthesis. At the top, a zoomed view of selected regions of the patterns; the intensities of the interval 29−33° are reduced by a factor of 0.7 with respect to those of the 21−25° range.

Table 1. Cell Parameters and Coherence Lengths Evaluated from the Width at Half-Maximum Intensity of the (*2 0 1*) Reflection of the α-TCP Pattern

	a (Å)	*b* (Å)	*c* (Å)	β (°)	*V* (Å^3)[a]	τ_{201} (nm)
α-TCP	12.887(4)	27.280(5)	15.219(2)	126.20(1)	4317.5	98(2)
Sr2	12.859(3)	27.363(4)	15.229(3)	126.25(1)	4321.2	117(3)
Sr4	12.853(2)	27.407(4)	15.240(4)	126.19(1)	4332.5	114(3)
Sr6	12.856(2)	27.451(4)	15.250(3)	126.13(2)	4346.6	115(3)
Sr8	12.853(3)	27.486(3)	15.257(3)	126.07(3)	4356.7	116(3)
Sr10	12.863(2)	27.536(5)	15.276(3)	126.02(3)	4376.0	117(3)
α-TCP-D	12.883(3)	27.275(5)	15.215(3)	126.22(1)	4312.8	94(2)
Sr10-D	12.865(4)	27.536(6)	15.275(5)	126.02(3)	4376.3	104(3)

[a]e.s.d. lower than 0.1.

https://doi.org/10.1021/acs.cgd.3c00358
Cryst. Growth Des. 2023, 23, 5690−5698

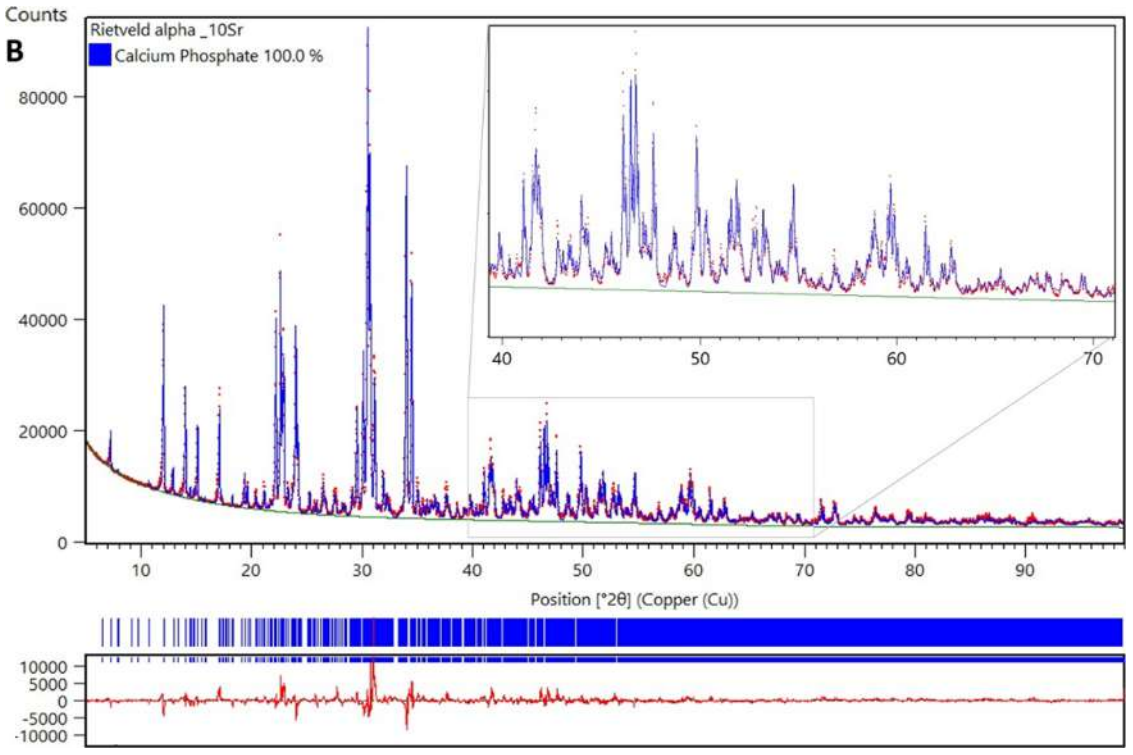

Figure 3. Comparison of the observed (red dots) and calculated (blue line) patterns of the Sr10 sample. Vertical bars are reflection markers of α-TCP structure; the curve difference is reported.

Table 2. Refined OFs, Overall Strontium Content, and Reliability Rwp Factor for Sr6 and Sr10 Samples

	Sr6		Sr10	
	Sr OF/Sr atoms per unit cell		Sr OF/Sr atoms per unit cell	
M(1)[a]	0	0	0	0
M(2)	0	0	0.06(1)	0.24(4)
M(3)	0.05(2)	0.20(8)	0.06(1)	0.24(4)
M(4)	0.02(1)	0.08(4)	0.01(1)	0.04(4)
M(5)	0.20(3)	0.8(1)	0.29(3)	1.2(1)
M(6)	0.02(1)	0.08(4)	0.10(2)	0.40(8)
M(7)	0	0	0	0
M(8)	0	0	0.10(3)	0.4(1)
M(9)	0	0	0	0
M(10)	0.10(3)	0.4(1)	0.10(3)	0.4(1)
M(11)	0.23(4)	0.9(2)	0.35(4)	1.4(2)
M(12)	0	0	0	0
M(13)	0	0	0	0
M(14)	0.10(2)	0.40(8)	0.10(3)	0.4(1)
M(15)	0	0	0.10(3)	0.4(1)
M(16)	0	0	0.05(1)	0.20(4)
M(17)	0.38(3)	1.5(1)	0.50(3)	2.0(1)
M(18)	0	0	0	0
Sr atom/cell	4.4(7)		7(1)	
metal atom/cell	72		72	
Sr atom %	6.1(9)		10.1(4)	
Rwp %	9.7		9.2	

[a]Multiplicity of all metal sites in α-TCP structure is 4.

results, providing Sr-substituted α-TCP just up to 10 at % of strontium. As a further reference for the samples prepared by *1-step* synthesis, pure α-TCP was synthesized by the direct solid-state reaction at 1300 °C between $CaCO_3$ and $CaHPO_4 \cdot 2H_2O$.[10] The XRD patterns of α-TCP and Sr10 prepared by *1-step* and *2-step* syntheses are compared in Figure 2.

Although the values of the lattice constants display just minor differences as a function of the method of synthesis, small but appreciable variations can be detected in the sharpness of the XRD reflections and, as a consequence, in the dimensions of the coherence length of the perfect crystalline domains, which are slightly smaller for the products obtained through 1-step synthesis (Table 1).

Figure S2 reports the SEM micrographs of some of the products: both *1-step* and *2-steps* α-TCP appear constituted of big dense blocks characterized by rounded edges and presence of holes. The products obtained in the presence of Sr display SEM images where the blocks appear fragmented and exhibit more sharp edges, independently from the method of synthesis.

Structural Analysis. To gain deeper insight into structural details, Rietveld refinements were carried out on samples Sr6 and Sr10 by using the monoclinic structure of α-TCP reported in the literature.[2] The procedure followed usual steps, but in the last cycles, the occupancy factors (OF) of calcium were left free to vary. In sites where occupancy exceeded unity, strontium atoms were added at the same calcium positions with the constraint $OF_{Ca} + OF_{Sr} = 1$. At variance, no substitution with strontium was considered in the final refinement in sites with the refined calcium OF equal to one, within standard deviation. Because of the correlation of the OF with thermal parameters, these were fixed at the values previously reported in the structure,[2] but an overall thermal parameter was introduced. No constraint was imposed on the overall strontium content. In consideration of the very small expansion of the unit cell caused by ionic substitution and of the huge number of atoms in the α-TCP structural unit (18 calcium and 12 phosphorus), the atom positions were kept fixed.

https://doi.org/10.1021/acs.cgd.3c00358
Cryst. Growth Des. 2023, 23, 5690−5698

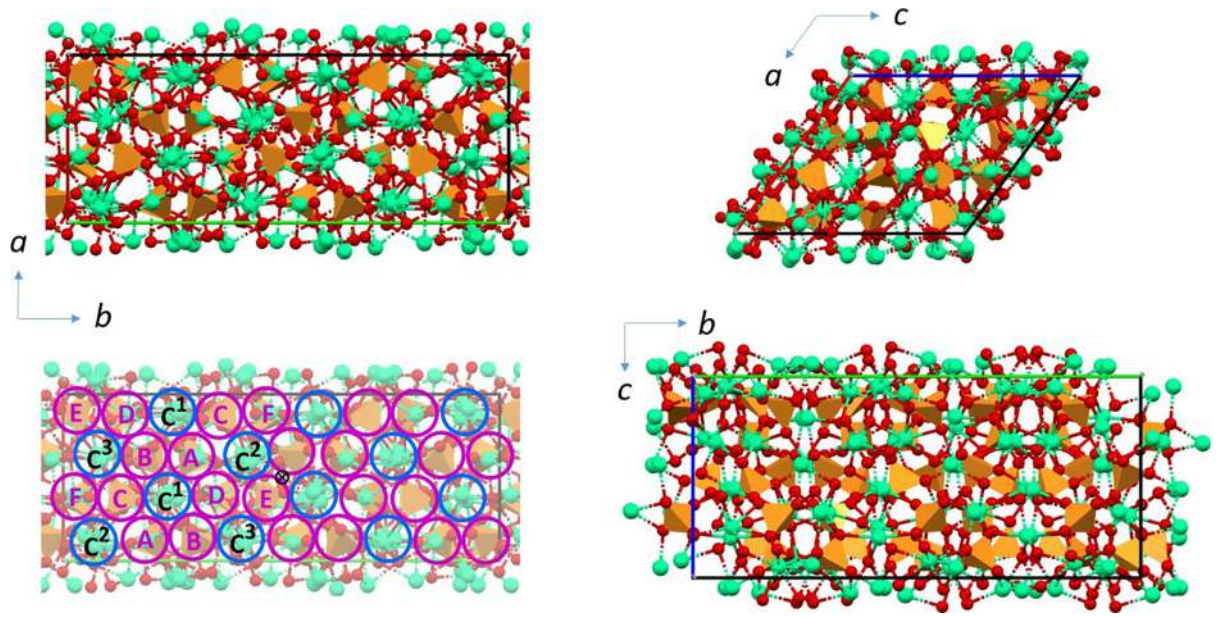

Figure 4. Views of the α-TCP structure projected perpendicular to the crystallographic axes. Along the c axis, it is possible to identify cation−cation columns (blue circles) surrounded by cation−anion columns (magenta circles). Three cation−cation columns are identified based on Ca sites contained in each one; in C1 are accommodated Ca8, 9, 10, 11; in C2 are found Ca2, 3, 4, 5; in C3 are contained Ca14, 15, 16, 17. Six different distributions of calcium and phosphate ions are present in cation−anion columns; in A Ca7, P3, P4; in B Ca12, P5, P6; in C Ca6, P1, P2; in D Ca13, P7, P8; in E Ca18, P9, P10; in F Ca1, P11, P12. The cross is the center of symmetry. Plots created with Mercury software (CCDC, rev. 2022.3.0).

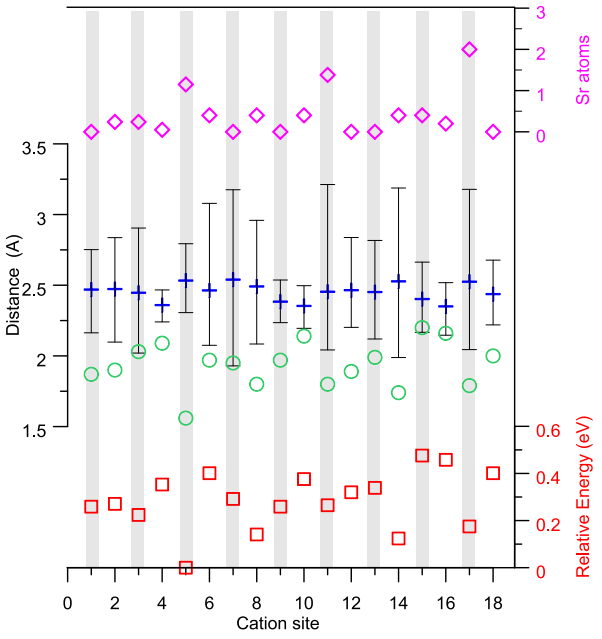

Figure 5. Sr10 average Ca−O distances (cross), bond valence sums (circles), and interval of bond distances (vertical bars) for each of the 18 cation sites in the α-TCP structure (distances less than 3.0 Å are considered). The number of Sr atoms at each site is shown (diamonds). Squares indicate the relative total energies of Sr at the different cation sites of α-TCP, as reported in ref 12.

A Rietveld plot for the refinement of sample Sr10 is reported in Figure 3 as an example (plot of sample Sr6 in Figure S3), whereas the most relevant structural parameters are reported in Table 2. The small discrepancies between the observed and calculated patterns reported in Figure 3 can be due to a minor contaminant phase. However, the differences between the relative integrated intensities are less than 2% and do not significantly affect the results. The overall strontium contents resulted similar to the amounts utilized in the syntheses. Furthermore, structural refinements indicate that strontium substitution is highly specific both in Sr6 and in Sr10 samples (please see Table 2). Indeed, strontium substitutes for calcium only at peculiar cation sites. In particular, more than 60% of overall strontium atoms are located at three sites, namely, M(17), M(11), and M(5), with minor substitution at several other sites. The nonhomogeneous distribution of strontium in the different cation sites justifies the different influence of the ion on the position of the diffraction maxima (Figure 1) and, as a consequence, on the values of the lattice constants (Figure S1).

Figure 4 reports the α-TCP structure projected perpendicular to the crystallographic axes. As outlined in the caption, the structure includes three kinds of C−C columns accommodating 12 calcium sites and 4 in each column. On the other hand, just one calcium site is accommodated in each one of the six different C−A columns. Strontium substitution involves mostly sites in the C−C columns and almost no substitution in C−A columns, with the exception of a small amount in (M6). In particular, in both Sr6 and Sr10 samples, strontium is spread in all the three

Table 3. Crystalline Phases Present in the Powder X-ray Diffraction Patterns of the Products Obtained after Different Periods of Sample Storage in H_3PO_4 Solution at 25 °C[a]

sample	15 h	24 h	48 h	72 h	96 h	5 days	7 days
α	α	α	α + O	O + α	O + α	O	O
α-D	α	O	O	O	O	O	O
Sr2	α	α	α	α	α	O + α	O
Sr6	α	α	α	α	α	α + O	O
Sr10	α	α	α	α	α	α	α
Sr10-D	α	α	α	α	α + O	O + α	O + α

[a]In the case of the co-presence of more than one crystalline phase, the different phases are reported starting from the most abundant one. Symbols: α = α-TCP; O = OCP.

https://doi.org/10.1021/acs.cgd.3c00358
Cryst. Growth Des. 2023, 23, 5690−5698

Table 4. Crystalline Phases Present in the Powder X-ray Diffraction Patterns of the Products Obtained after Different Periods of Sample Storage in H_3PO_4 Solution at 60 °C[a]

sample	3 h	6 h	9 h	15 h	24 h	48 h	72 h
α	α	α + O	O + α	O + H	H	H	H
α-D	α	α + H	H	H	H	H	H
Sr2	α	α	α + O	α + O	H + O	H	H
Sr6	α	α	α + O	α + O	O + α	O + H	H + O + α
Sr10	α	α	α + O	α + O	O + α	O + α	
Sr10-D	α	O + α	O + α	O + α	O + α + H	H + O	H + β

[a]In the case of the co-presence of more than one crystalline phase, the different phases are reported starting from the most abundant one. Symbols: α = α-TCP; O = OCP; H = HA, β = β-TCP.

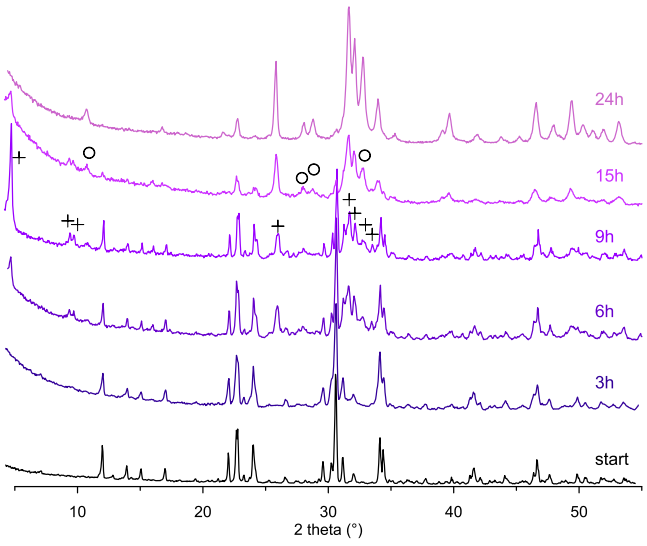

Figure 6. XRD patterns of the time course of hydrolysis at 60 °C in H_3PO_4 solution of α-TCP obtained through *2-step* synthesis. Crosses indicate characteristic OCP peaks, and circles indicate HA.

C−C columns with the highest content in C^3 and the lowest in C^2. Similarly, preferential substitution of barium for sites M(17), M(11), and M(5) was previously reported for three samples of Ba-doped α-TCP structure and ascribed to the relatively small bond valence sums (BVS) of these positions.[31]

Figure 5 reports the distribution of strontium in the different cation sites, average Ca−O bond distances, bond distances intervals, and BVS for the full set of calcium positions of Sr10. Sites 17, 11, and 5 exhibit the concomitant presence of relatively low BVS, long mean Ca−O distance, and wide Ca−O distance distribution. Furthermore, these sites are among those energetically preferred on the basis of theoretical calculations carried out by Matsunaga et al. on divalent cations substituting for calcium in α-TCP, as shown in Figure 5.[12] Other cationic sites share these characteristics but display a significant lower occupancy. On considering cation distribution in the different columns, it could be suggested that C−C columns cannot host more than one cation site containing strontium. The present experimental data provide a further confirmation that local arrangements are driven by thermodynamic stability and surrounding environments.

Hydrolysis. The analysis of the products of the hydrolysis carried out under different conditions puts in evidence the effect of different parameters on this process. First of all, the results of the XRD analysis confirm the role of temperature in the conversion of α-TCP: the comparison of the data obtained in H_3PO_4 solution at 25 and at 60 °C shows that α-TCP conversion into OCP (ICDD PDF 00-026-1056) starts after just 6 h at 60 °C, whereas it needs about 48 h of immersion at 25 °C. Moreover, 24 h at 60 °C are enough to get complete conversion into HA (ICDD PDF 01-074-0566), while at 25 °C, the conversion is limited to OCP even after 7 days (Tables 3 and 4). The time course of α-TCP hydrolysis at 60 °C in H_3PO_4 solution is illustrated by the XRD patterns reported in Figure 6.

The environment is a further important parameter: at the same temperature, 60 °C, the products of conversion obtained in phosphoric acid are different from those obtained in physiological solution. In particular, the presence of OCP is appreciable just after storage in H_3PO_4 solution, whereas in NaCl, the conversion yields directly HA. The presence of OCP during hydrolysis in H_3PO_4 solution can be ascribed to the slightly acidic conditions and to the presence of phosphoric acid, in agreement with previous data.[10,32,33] The process of hydrolysis is slowed down by the presence of strontium inside the crystal structure of α-TCP: Sr-substituted samples require several days in H_3PO_4 solution at 25 °C to partially convert into OCP, a conversion that is completely inhibited for Sr10 (Table 3). Similarly, Sr slows down the conversion into HA in saline solution at 60 °C (Table 5), whereas the conversion into HA is not complete even after 72 h in H_3PO_4 at 60 °C for the samples

Table 5. Crystalline Phases Present in the Powder X-ray Diffraction Patterns of the Products Obtained after Different Periods of Sample Storage in NaCl Solution at 60 °C[a]

sample	3 h	6 h	9 h	15 h	24 h	48 h	72 h
α	α	α	H + α	H	H	H	H
α-D	α	α + H	H	H	H	H	H
Sr2	α	α	α	α	H	H	H
Sr6	α	α	α	α	α + H	H + α	H
Sr10	α	α	α	α	α	H + α	H + β
Sr10-D	α	α	α	α + H	α + H	H	H + β

[a]In the case of the co-presence of more than one crystalline phase, the different phases are reported starting from the most abundant one. Symbols: α = α-TCP; H = HA, β = β-TCP.

https://doi.org/10.1021/acs.cgd.3c00358
Cryst. Growth Des. 2023, 23, 5690−5698

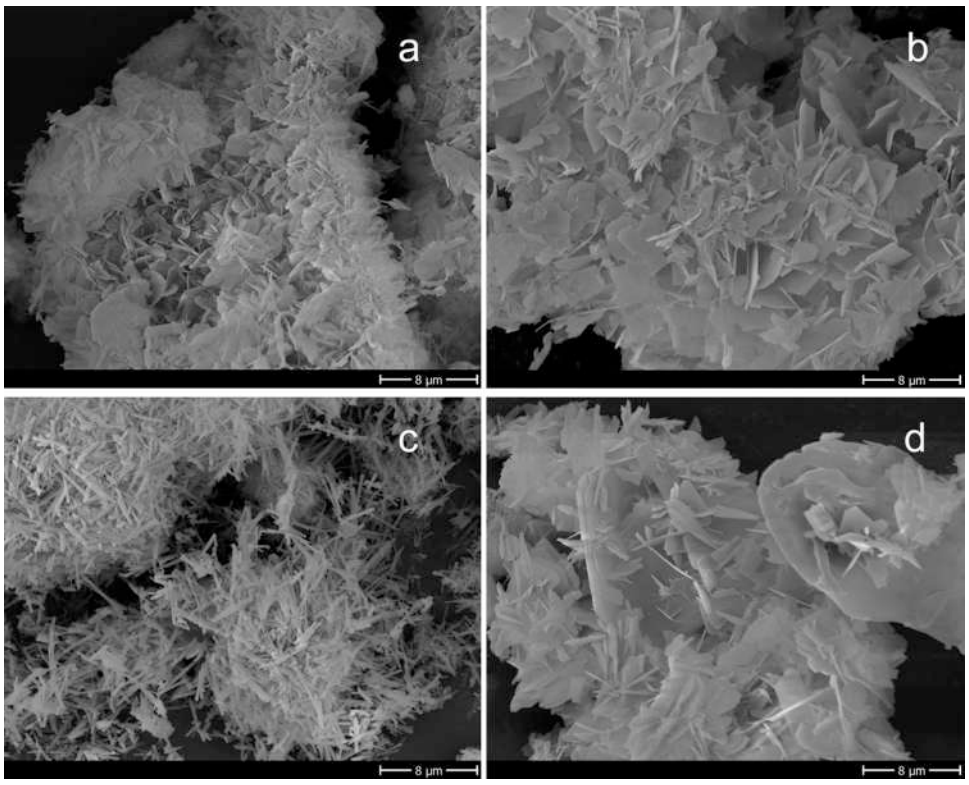

Figure 7. SEM images of the products obtained from the hydrolysis reaction of α-TCP in physiological solution at 60 °C after 72 h (a) or in H_3PO_4 at 25 °C after 7 days (b) and of Sr10 in physiological solution at 60 °C (c) or in H_3PO_4 at 60 °C (d) after 72 h. Magnification in all the images is the same for direct comparison.

at a relatively high Sr content (Table 4). A peculiar result obtained for the processes carried out at 60 °C is the presence of very small, but appreciable, amounts of β-TCP in the products obtained through hydrolysis of the samples at a high Sr content.

Also, the method of synthesis influences the time course of the hydrolysis products: the samples obtained through the *1-step* process undergo a faster hydrolysis in comparison with those obtained through a *2-step* route, as shown by the results reported in Tables 3−5 for α-TCP-D and Sr10-D: the conversion is slower for Sr10-D than for α-TCP-D, but both of them convert earlier than their *2-steps* analogues. These data are in agreement with the values of the coherence length of the perfect crystalline domains reported in Table 1, which indicate a smaller crystallite size of the products of *1-step* synthesis. The smaller crystallite size indicates less perfection of the crystal structure. Moreover, these materials are less stable in solution, as shown by the data obtained on Ca release in NaCl at 60 °C: the amount of calcium released from α-TCP-D after 5 h is significantly greater than that released from α-TCP (Figure S4). Since the transformation in solution of α-TCP into more stable phases occurs through a dissolution/precipitation process,[32] it is not surprising that the lower stability and higher solubility of the products of *1-step* synthesis result in a faster transformation.

Further interesting results are given by the values of the lattice constants of OCP and HA obtained through hydrolysis and reported in Table S1: it is evident that the phases obtained from Sr-substituted samples exhibit enlarged cell parameters in comparison to those obtained through hydrolysis of pure α-TCP, in agreement with Sr incorporation into these structures.

Figure 7 shows the different morphologies of hydrolysis products: materials converted into OCP are constituted of platelike crystals clustered in spherulites (Figure 7b), whereas much smaller crystals, which in the presence of strontium appear needle-like, can be appreciated in the images of samples made of HA (Figure 7a,c). The co-presence of OCP and HA characteristic morphologies is shown in sample Sr10 in H_3PO_4 solution at 60 °C for 72 h (Figure 7d).

CONCLUSIONS

The results of this study indicate that Sr can enter into the α-TCP structure up to about 10 at %, independently from the high-temperature synthesis route. Strontium substitution for calcium is testified by the enlargement of the cell volume and provokes a slight increase of the values of the coherent length of the perfect crystalline domains and minor modifications of the morphology. The products obtained through *2-step* and *1-step* syntheses are similar, apart from small differences in crystallinity and stability in solution. However small, these differences influence the hydrolysis process so that the conversion into more stable phases of the samples obtained through *1-step* synthesis proceeds faster than that of the products of *2-step* synthesis. Hydrolysis depends also on temperature and Sr content: temperature accelerates the process, whereas Sr presence slows it down. The products of hydrolysis are OCP, which is obtained just in a mildly acidic H_3PO_4 solution, and HA, directly obtained in physiological solution: both of them exhibit lattice parameters coherent with a partial substitution of Sr for Ca in their structures.

Rietveld refinements indicate that Sr replacement to Ca in α-TCP structure occurs preferentially at specific sites: mostly at three cation sites, each located at a different cation−cation column, characterized by relatively low BVS, long mean Ca−O distances, and wide Ca−O distance distribution. The not homogeneous occupancy of Sr in the different cation sites is the

https://doi.org/10.1021/acs.cgd.3c00358
Cryst. Growth Des. 2023, 23, 5690−5698

reason of different shifts of the different X-ray diffraction maxima and of the different variations of the lattice constants as a function of the Sr content.

The results of this study provide a further tile of information in the knowledge of ionic substitution in calcium phosphates, which is also useful for controlling the properties of the synthesized phase, as well as for delivery of bioactive ions when calcium phosphates are utilized in biomedical applications. In particular, the amount of strontium, as well as the synthetic method, could be used to tune the hydrolysis process of α-TCP.

■ ASSOCIATED CONTENT

Supporting Information

The Supporting Information is available free of charge at https://pubs.acs.org/doi/10.1021/acs.cgd.3c00358.

Plot of cell parameters of strontium-substituted α-TCP samples; SEM images of the as-prepared samples; final plot of Rietveld structural refinement for Sr6; plot of calcium release; and cell parameters of crystal phases obtained after the hydrolysis process (PDF)

■ AUTHOR INFORMATION

Corresponding Author

Elisa Boanini − *Department of Chemistry "Giacomo Ciamician", Alma Mater Studiorum − University of Bologna, Bologna 40126, Italy;* orcid.org/0000-0003-3754-0273; Email: elisa.boanini@unibo.it

Authors

Massimo Gazzano − *ISOF-CNR, Bologna 40129, Italy;* orcid.org/0000-0003-1352-9547

Katia Rubini − *Department of Chemistry "Giacomo Ciamician", Alma Mater Studiorum − University of Bologna, Bologna 40126, Italy*

Adriana Bigi − *Department of Chemistry "Giacomo Ciamician", Alma Mater Studiorum − University of Bologna, Bologna 40126, Italy*

Complete contact information is available at: https://pubs.acs.org/10.1021/acs.cgd.3c00358

Author Contributions

The manuscript was written through contributions of all authors. All authors have given approval to the final version of the manuscript.

Funding

This research received no external funding.

Notes

The authors declare no competing financial interest.

■ ACKNOWLEDGMENTS

The authors are grateful to the support of the University of Bologna.

■ REFERENCES

(1) Dickens, B.; Schroeder, L. W.; Brown, W. E. Crystallographic studies of the role of Mg as a stabilizing impurity in β-$Ca_3(PO_4)_2$. The crystal structure of pure β-$Ca_3(PO_4)_2$. *J. Solid State Chem.* **1974**, *10*, 232−248.

(2) Mathew, M.; Schroeder, L. W.; Dickens, B.; Brown, W. E. The crystal structure of α-$Ca_3(PO_4)_2$. *Acta Crystallogr., Sect. B: Struct. Sci., Cryst. Eng. Mater.* **1977**, *33*, 1325−1333.

(3) Carrodeguas, R. G.; De Aza, S. α-Tricalcium phosphate: Synthesis, properties and biomedical applications. *Acta Biomater.* **2011**, *7*, 3536−3546.

(4) Torres, P. M. C.; Abrantes, J. C. C.; Kaushal, A.; Pina, S.; Döbelin, N.; Bohner, M.; Ferreira, J. M. F. Influence of Mg-doping, calcium pyrophosphate impurities and cooling rate on the allotropic $\alpha\leftrightarrow\beta$-tricalcium phosphate phase transformations. *J. Eur. Ceram. Soc.* **2016**, *36*, 817−827.

(5) Bohner, M.; Le Gars Santoni, B.; Döbelin, N. β-tricalcium phosphate for bone substitution: Synthesis and properties. *Acta Biomater.* **2020**, *113*, 23−41.

(6) Tronco, M. C.; Cassel, J. B.; dos Santos, L. A. α-TCP-based calcium phosphate cements: A critical review. *Acta Biomater.* **2022**, *151*, 70−87.

(7) Bigi, A.; Cojazzi, G.; Panzavolta, S.; Ripamonti, A.; Roveri, N.; Romanello, M.; Noris Suarez, K.; Moro, L. Chemical and structural characterization of the mineral phase from cortical and trabecular bone. *J. Inorg. Biochem.* **1997**, *68*, 45−51.

(8) Li, J.; Deng, C.; Liang, W.; Kang, F.; Bai, Y.; Ma, B.; Wu, C.; Dong, S. Mn-containing bioceramics inhibit osteoclastogenesis and promote osteoporotic bone regeneration via scavenging ROS. *Bioact. Mater.* **2021**, *6*, 3839−3850.

(9) Dorozhkin, S. V.; Epple, M. Biological and medical significance of calcium phosphates. *Angew. Chem., Int. Ed.* **2002**, *41*, 3130−3146.

(10) Boanini, E.; Panzavolta, S.; Rubini, K.; Gandolfi, M.; Bigi, A. Effect of strontium and gelatin on the reactivity of α-tricalcium phosphate. *Acta Biomater.* **2010**, *6*, 936−942.

(11) O'Neill, R.; McCarthy, H. O.; Montufar, E. B.; Ginebra, M. P.; Wilson, D. I.; Lennon, A.; Dunne, N. Critical review: Injectability of calcium phosphate pastes and cements. *Acta Biomater.* **2017**, *50*, 1−19.

(12) Matsunaga, K.; Kubota, T.; Toyoura, K.; Nakamura, A. First-principles calculations of divalent substitution of Ca2+ in tricalcium phosphates. *Acta Biomater.* **2015**, *23*, 329−337.

(13) Cicek, G.; Aksoy, E. A.; Durucan, C.; Hasirci, N. Alpha-tricalcium phosphate (α-TCP): solid state synthesis from different calcium precursors and the hydraulic reactivity. *J. Mater. Sci.: Mater. Med.* **2011**, *22*, 809−817.

(14) Martinez, T.; Espanol, M.; Charvillat, C.; Marsan, O.; Ginebra, M. P.; Rey, C.; Sarda, S. α-tricalcium phosphate synthesis from amorphous calcium phosphate: structural characterization and hydraulic reactivity. *J. Mater. Sci.* **2021**, *56*, 13509−13523.

(15) Brazete, D.; Torres, P. M. C.; Abrantes, J. C. C.; Ferreira, J. M. F. Influence of the Ca/P ratio and cooling rate on the allotropic $\alpha\leftrightarrow\beta$-tricalcium phosphate phase transformations. *Ceram. Int.* **2018**, *44*, 8249−8256.

(16) Enderle, R.; Götz-Neunhoeffer, F.; Göbbels, M.; Müller, F. A.; Greil, P. Influence of magnesium doping on the phase transformation temperature of β-TCP ceramics examined by Rietveld refinement. *Biomaterials* **2005**, *26*, 3379−3384.

(17) Gallo, M.; Le Gars Santoni, B.; Douillard, T.; Zhang, F.; Gremillard, L.; Dolder, S.; Hofstetter, W.; Meille, S.; Bohner, M.; Chevalier, J.; Tadier, S. Effect of grain orientation and magnesium doping on β-tricalcium phosphate resorption behavior. *Acta Biomater.* **2019**, *89*, 391−402.

(18) Xue, W. C.; Dahlquist, K.; Banerjee, A.; Bandyopadhyay, A.; Bose, S. Synthesis and characterization of tricalcium phosphate with Zn and Mg based dopants. *J. Mater. Sci.: Mater. Med.* **2008**, *19*, 2669−2677.

(19) Jegou Saint-Jean, S.; Camiré, C. L.; Nevsten, P.; Hansen, S.; Ginebra, M. P. Study of the reactivity and in vitro bioactivity of Sr-substituted α-TCP cements. *J. Mater. Sci.: Mater. Med.* **2005**, *16*, 993−1001.

(20) Yuan, Z.; Bi, J.; Wang, W.; Sun, X.; Wang, L.; Mao, J.; Yang, F. Synthesis and properties of Sr^{2+} doping α-tricalcium phosphate at low temperature. *J. Appl. Biomater. Funct. Mater.* **2021**, *19*, No. 2280800021996999.

(21) Christensen, T. E. K.; Davidsen, M. B.; Van Malderen, S.; Garrevoet, J.; Offermanns, V.; Andersen, O. Z.; Foss, M.; Birkedal, H. Local release of strontium from sputter-deposited coatings at implants

increases the strontium-to-calcium ratio in peri-implant bone. *ACS Biomater. Sci. Eng.* **2022**, *8*, 620−625.
(22) Boanini, E.; Torricelli, P.; Gazzano, M.; Della Bella, E.; Fini, M.; Bigi, A. Combined effect of strontium and zoledronate on hydroxyapatite structure and bone cell responses. *Biomaterials* **2014**, *35*, 5619−5626.
(23) Lode, A.; Heiss, C.; Knapp, G.; Thomas, J.; Nies, B.; Gelinsky, M.; Schumacher, M. Strontium-modified premixed calcium phosphate cements for the therapy of osteoporotic bone defects. *Acta Biomater.* **2018**, *65*, 475−485.
(24) Salamanna, F.; Giavaresi, G.; Contartese, D.; Bigi, A.; Boanini, E.; Parrilli, A.; Lolli, R.; Gasbarrini, A.; Barbanti Brodano, G.; Fini, M. Effect of strontium substituted ß-TCP associated to mesenchymal stem cells from bone marrow and adipose tissue on spinal fusion in healthy and ovariectomized rat. *J. Cell. Physiol.* **2019**, *234*, 20046−20056.
(25) Boanini, E.; Pagani, S.; Tschon, M.; Rubini, K.; Fini, M.; Bigi, A. Monetite vs. Brushite: Different influences on bone cell response modulated by strontium functionalization. *J. Funct. Biomater.* **2022**, *13*, 65.
(26) Aina, V.; Bergandi, L.; Lusvardi, G.; Malavasi, G.; Imrie, F. E.; Gibson, I. R.; Cerrato, G.; Ghigo, D. Sr-containing hydroxyapatite: morphologies of HA crystals and bioactivity on osteoblast cells. *Mater. Sci. Eng. C* **2013**, *33*, 1132−1142.
(27) Boanini, E.; Torricelli, P.; Fini, M.; Bigi, A. Osteopenic bone cell response to strontium-substituted hydroxyapatite. *J. Mater. Sci.: Mater. Med.* **2011**, *22*, 2079−2088.
(28) Capuccini, C.; Torricelli, P.; Boanini, E.; Gazzano, M.; Giardino, R.; Bigi, A. Interaction of Sr-doped hydroxyapatite nanocrystals with osteoclast and osteoblast-like cells. *J. Biomed. Mater. Res., Part A* **2009**, *89A*, 594−600.
(29) Boanini, E.; Gazzano, M.; Nervi, C.; Chierotti, M. R.; Rubini, K.; Gobetto, R.; Bigi, A. Strontium and zinc substitution in β-tricalcium phosphate: An X-ray diffraction, solid state NMR and ATR-FTIR study. *J. Funct. Biomater.* **2019**, *10*, 20.
(30) Brese, N. E.; O'Keeffe, M. Bond-valence parameters for solids. *Acta Crystallogr., Sect. B: Struct. Sci., Cryst. Eng. Mater.* **1991**, *47*, 192−197.
(31) Yashima, M.; Kawaike, Y. Crystal structure and site preference of Ba-doped α-tricalcium phosphate $(Ca_{1-x}Ba_x)_3(PO_4)_2$ through high-resolution synchrotron powder diffraction (x = 0.05 to 0.15). *Chem. Mater.* **2007**, *19*, 3973−3979.
(32) Bigi, A.; Boanini, E.; Botter, R.; Panzavolta, S.; Rubini, K. α-tricalcium phosphate hydrolysis to octacalcium phosphate: effect of sodium polyacrylate. *Biomaterials* **2002**, *23*, 1849−1854.
(33) Kovrlija, I.; Menshikh, K.; Marsan, O.; Rey, C.; Combes, C.; Locs, J.; Loca, D. Exploring the formation kinetics of octacalcium phosphate from alpha-tricalcium phosphate: synthesis scale-up, determination of transient phases, their morphology and biocompatibility. *Biomolecules* **2023**, *13*, 462.

https://doi.org/10.1021/acs.cgd.3c00358
Cryst. Growth Des. 2023, 23, 5690−5698